C. C. Yañez[1]*, F. M. Hopkins[2], X. Xu[1], J. F. Tavares[1], A. Welch[1], and C. I. Czimczik[1]*

[1]Department of Earth System Science, University of California Irvine, CA, USA 92697-3100

[2]Department of Environmental Sciences, University of California Riverside, CA, USA 92521

*Corresponding authors: Cindy Yañez (`ccyanez@uci.edu`), Claudia Czimczik (`czimczik@uci.edu`)

Key Points

- With COVID-19 restrictions, carbon dioxide enhancements on Los Angeles freeways were reduced by 60% in July 2020 relative to 2019

- Radiocarbon measurements of plants captured differences in fossil fuel carbon dioxide levels in urban California related to local pandemic measures

- Mobile and plant-based measurements of fossil fuel carbon dioxide can verify decarbonization progress in cities

Abstract

Fossil fuel CO_2 emissions ($ffCO_2$) constitute the majority of greenhouse gas emissions and are the main determinant of global climate change. The COVID-19 pandemic caused wide-scale disruption to human activity and provided an opportunity to evaluate our capability to detect $ffCO_2$ emission reductions. Quantifying changes in $ffCO_2$ levels is especially challenging in cities, where climate mitigation policies are being implemented but local emissions lead to spatially and temporally complex atmospheric mixing ratios. Here, we used direct observations of on-road CO_2 mole fractions with analyses of the radiocarbon (^{14}C) content of annual grasses collected by community scientists in Los Angeles and California, USA to assess reductions in $ffCO_2$ emissions during the first two years of the COVID-19 pandemic. With COVID-19 mobility restrictions in place in 2020, we observed a significant reduction in $ffCO_2$ levels across California, especially in urban centers. In Los Angeles, CO_2 enhancements on freeways were $60 \pm 16\%$ lower and $ffCO_2$ levels were 43-55% lower than in pre-pandemic years. By 2021, California's ffCO2 levels rebounded to pre-pandemic levels, albeit with substantial spatial heterogeneity related to local and regional pandemic measures. Taken together, our results indicate that a reduction in traffic emissions by ~60% (or 10-24% of Los Angeles' total $ffCO_2$ emissions) can be robustly detected by plant ^{14}C analysis and pave the way for mobile- and plant-based monitoring of $ffCO_2$ in cities without CO_2 monitoring infrastructure such as those in the Global South.

Plain language summary

Cities emit large amounts of greenhouse gases, especially fossil fuel-derived carbon dioxide ($ffCO_2$), and thus contribute to climate change. Reducing emissions is challenging because it is difficult to quantify the many and variable $ffCO_2$ sources of individual neighborhoods and cities. Here, we measured $ffCO_2$ reductions during the COVID-19 pandemic, demonstrating that two measurement approaches are sensitive enough to detect changes in $ffCO_2$ at fine spatial scales. We measured CO_2 levels on Los Angeles freeways using a mobile laboratory and analyzed the isotopic content of plant species collected by community scientists across the state of California. Both analyses indicate substantial reductions in fossil fuel emissions in 2020 during California's pandemic-related shift to remote work and varying degrees of emission rebounds by 2021. We found that measurements of radiocarbon in plants is particularly sensitive to local-scale changes in human activity. Our results demonstrate that measuring the radiocarbon content of plants can serve as a powerful, cost-effective approach to quantify changes in cities' $ffCO_2$ patterns and monitor decarbonization as climate agreements take effect. Further development and implementation of these methods could significantly improve our shared capacity to address climate change, particularly in cities of the Global South which often lack CO_2 monitoring infrastructure.

1 Introduction

Carbon dioxide (CO_2) emissions associated with fossil fuel consumption ($ffCO_2$) are the dominant cause of climate change. Hence, there is an urgent need to quantify $ffCO_2$ emissions to support the success of climate change mitigation efforts. Urban areas account for 30-84% of global $ffCO_2$ emissions (Seto et al., 2014), despite encompassing less than 1% of the Earth's land area (Zhou et al., 2015). While being disproportional contributors to climate change, cities are also at the forefront of climate change mitigation actions (Rosenzweig et al., 2010), making them a top priority for quantifying and monitoring $ffCO_2$ emission reduction efforts. However, atmospheric observation systems are limited in their ability to detect trends in $ffCO_2$ at the neighborhood scale that is needed to inform local policy makers on the outcome of mitigation actions (Duren & Miller, 2012).

The abrupt halt of economic activity at the beginning of the COVID-19 pandemic (with strictest regulations in March to May of 2020 in the U.S.) provided an unplanned experiment on the sensitivity of atmospheric greenhouse gas (GHG) observations to changes in human behavior. Restrictions intended to prevent the spread of the virus caused a wide scale disruption of human activities and consequently the largest reduction in global $ffCO_2$ emissions than has ever been observed, inducing rapid emission reductions larger than any historical human crisis or climate agreement (Le Quéré et al., 2021). Several studies quantified these emission reductions using activity-based models ("bottom up" estimates) that scale sector-based activity and consumption data with CO_2 emission coefficients. One study calculated a 17% reduction in daily global

ffCO$_2$ emissions in April 2020 relative to 2019, based on a compilation of activity data and information on the intensity of mandated lockdowns (Le Quéré et al., 2020). Hourly to daily activity data indicated an overall global ffCO$_2$ decline of 8% in the first half of 2020 relative to 2019 (Liu et al., 2020). Pandemic related emission reductions have also been assessed using atmospheric observations ("top-down" estimates), such as measurements of the total CO$_2$ mixing ratio by in situ tower observation networks. One such study reported a 30% reduction in the San Francisco Bay Area's CO$_2$ levels during the first six weeks of California's statewide Stay-At-Home Order (March 22 to May 4, 2020) relative to the six weeks before the order (Turner et al., 2020a). Similar (~30%) reductions were reported for the Los Angeles (LA) and Washington DC/Baltimore metropolitan areas in April 2020 relative to the previous two years (Yadav et al., 2021). Pandemic-related emission reductions were also observed in some remotely sensed data. One study combined bottom-up estimates and observations of nitrogen oxides (NO$_x$, pollutants that are co-emitted with CO$_2$ during fossil fuel combustion) from the Tropospheric Monitoring Instrument (TROPOMI) to calculate a 12% decline in China's CO$_2$ emissions in the first four months of 2020 relative to 2019 (Zheng et al., 2020). However, studies analyzing data from CO$_2$-observing satellites (such as OCO-2 and GOSAT) could not conclusively detect pandemic-related emission reductions because of sparse data retrievals, low resolution, and weak signals (Buchwitz et al., 2021; Chevallier et al., 2020).

Quantifying ffCO$_2$ emission reductions (i.e., isolating fossil fuel contributions from the total CO$_2$ signal) remains a key challenge for climate change mitigation efforts, especially at localized spatial scales. This is because ffCO$_2$ emissions are superimposed on large and poorly constrained fluxes from land ecosystems (e.g., photosynthesis and respirations of plants and soil microorganisms) that vary seasonally and interannually in response to temperature, the timing and amount of precipitation, drought, fire, and management (irrigation, harvest) as well as emissions from biofuel combustion and human metabolism (e.g., respiration, sewage). Recent work in the LA metropolitan area revealed that biospheric emissions contribute a significant proportion (~30%) to the excess level of CO$_2$ observed in the urban atmosphere (Miller et al., 2020). Thus, an effective ffCO$_2$ monitoring system requires a direct way to isolate fossil fuel sources from other entangled CO$_2$ fluxes, high spatial resolution (neighborhood scale), and accessibility to global cities. Urban tower networks that continuously measure CO$_2$ levels are only established in a small selection of cities and largely absent in the growing economies of the Global South. Remote sensing data can provide global CO$_2$ observations but are not currently capable of monitoring ffCO$_2$ at the neighborhood scale, as they are typically designed to study regional scale CO$_2$ fluxes on the order of 1000 km^2 (Eldering et al., 2019). These satellites observe the total column abundance of CO$_2$ (XCO$_2$), and even high emitting cities only enhance the XCO$_2$ signal by approximately 6 ppm (Kiel et al., 2021; Schwandner et al., 2017) which is not much larger than the uncertainty in the instruments (1 ppm for OCO-2 and OCO-3), and are not able to separate ffCO$_2$ from biogenic fluxes. Complementary methods to quantify ffCO$_2$ at urban and

regional scales in places without existing high quality CO_2 monitoring infrastructure are urgently needed to ensure the success of mitigation efforts like the 2021 Glasgow Climate Pact.

Tracking the progress of urban decarbonization efforts requires data representing ffCO_2 emissions at the neighborhood scale that is accessible to global cities and can isolate fossil sources. Mobile surveys with GHG observatories can examine fine scale patterns in fossil fuel CO_2 emissions from vehicle sources in urban areas (Bush et al., 2015). Another powerful approach is the radiocarbon analysis of plants. Radiocarbon (^{14}C, a radioactive carbon isotope with a half-life of 5,730 years) can uniquely isolate CO_2 derived from fossil sources. Currently, an input of 1 ppm of ffCO_2 into the atmosphere results in a depletion of ambient $\Delta^{14}CO_2$ by 2.4‰. This is because fossil fuel-derived CO_2 is millions of years old and devoid of ^{14}C because of radioactive decay, while CO_2 from biogenic sources is enriched in ^{14}C due to the production of ^{14}C by natural and anthropogenic processes in the atmosphere and its incorporation into biomass during photosynthesis (Graven et al., 2020). Plants that grow in locations with high ffCO_2 emissions appear depleted in ^{14}C, or older in their ^{14}C age since ffCO_2 emissions dilute background ^{14}C in the atmosphere. Plants offer a natural and efficient network of ^{14}C observations and can be used to map fine-scale spatial patterns in ffCO_2 in places without established CO_2 monitoring infrastructure (Hsueh et al., 2007; Riley et al., 2008; Santos et al., 2019; Wang & Pataki, 2010). Many previous studies have measured the ^{14}C of ambient air to quantify ffCO_2 trends in urban areas (Miller et al., 2020; Newman et al., 2016; Turnbull et al., 2011); however, plants offer cost-effective, time-integrated monitoring of ^{14}C that could more feasibly be used to monitor ffCO_2 spatial patterns in global cities than deploying air sampling stations at the same scale. Evaluating the sensitivity of this approach to pandemic-induced ffCO_2 emission reductions could demonstrate its potential to monitor future changes in urban fossil fuel consumption, such as from decarbonization of global economies.

In this study, we quantify changes in ffCO_2 emissions during the first two years of the COVID-19 pandemic (2020 to 2021) in California, USA, with a focus on the state's two largest urban areas: the LA metropolitan area and the San Francisco Bay Area (SFBA). The State of California is the world's fifth largest economy and has enacted ambitious climate action goals that demand verification. Statewide policies that restricted mobility likely altered ffCO_2 emission patterns during the pandemic, such as the Stay-At-Home order that required the closing of all "non-essential" businesses from March 19 to May 4, 2020 (Executive Order N-33-20). To examine the impacts of these policies on ffCO_2 emissions, we use two approaches that can isolate CO_2 derived from fossil sources, are spatially resolved, and do not require establishment of CO_2 monitoring infrastructure. First, we measured the mixing ratio of CO_2 on freeways in the LA area using a mobile GHG observatory. These continuous on-road measurements are more sensitive to transportation-sector ffCO_2 emissions than tower networks or remote sensing products since they capture CO_2 enhancements at the source and are not as influenced by atmospheric transport. Second, we analyzed the

[14]C content of annual grasses collected by community scientists across the state. Together, our data offer a unique insight into anthropogenic ffCO$_2$ emissions in California's urban regions during the COVID-19 pandemic and establish ^{14}C analysis of annual plants as an effective method for evaluating decarbonization efforts.

2 Methods

2.1 On-road CO$_2$ measurements

We measured the on-road mixing ratios of CO$_2$ in the LA metropolitan area using a cavity ringdown spectrometer (Picarro Inc., Series G2401) installed inside a mobile laboratory (2016 Mercedes Sprinter cargo van). The same platform has been used by previous studies to observe GHG and pollutant concentrations (Carranza et al., 2022; Thiruvenkatachari et al., 2020). Ambient air was continuously pumped into the Picarro G2401 analyzer from an inlet on the ceiling of the van behind the driver's seat, roughly 3 m above the road surface. We simultaneously collected position and meteorological data using a global satellite positioning device (GPS 16X, Garmin Ltd.) and a compact weather sensor (METSENS500, Campbell Scientific, Inc.) that were mounted on the roof of the vehicle.

Measurements were collected on freeways during daytime hours on weekdays in July 2019, 2020, and 2021. We filtered the datasets from each year to only include locations that overlapped with the 2020 dataset, focusing the analysis on approximately 750 km of road. We only used data collected between 11 AM to 4 PM local time, when the planetary boundary layer is well-developed and surface layer air is well-mixed (Ware et al., 2016). We filtered out data from days that were overcast and otherwise experienced similar weather conditions during all three surveys.

We calibrated the analyzer using gas cylinders tied to the NOAA scale before and after each survey. For each calibration, the analyzer inlet was directed to sample air from compressed gas cylinders with known mixing ratios of CO$_2$ for three minutes. We used two standard tanks that spanned the range of CO$_2$ mixing ratios we observed on the road (Table S1). We then applied a two-point correction to the data based on the linear relationship between the known and measured values. The measured values were all within 2% of the known values. The calibrated data was aggregated into 5-second intervals and gridded into 100 m road segments to synchronize trace gas, weather, and position measurements.

Urban CO$_2$ enhancements (CO$_{2xs}$) were calculated by subtracting a background that represents the CO$_2$ mole fraction of air coming into the LA area. We characterized the CO$_2$ background using flask sample data from NOAA's Global Monitoring Division's site at Cape Kumukahi, Hawaii (19.54°N, 154.82°W, 15 m elevation). This data is publicly available at https://gml.noaa.gov/ (Dlugokencky et al., 2021). Previous work has found that this site is similar to the local LA background for summer months (Hopkins et al., 2016). Thus, we estimate the CO$_2$ background was 411.0 ± 2.0 ppm in 2019, 412.9 ± 1.2 ppm

in 2020, and 416.7 $\pm$ 1.7 ppm in 2021, based on the July average of all flask measurements at Cape Kumukahi. On July 31, 2020, we measured comparable CO_2 mixing ratios (413 $\pm$ 1.4 ppm) in the in-flowing marine air at Dockweiler Beach (33.94°N, -118.44°E), which supports the application of Cape Kumukahi as an adequate LA background.

2.2 Radiocarbon analysis of plants

We measured the ^{14}C content of invasive annual grasses to map $ffCO_2$ trends across the state of California. The typical growing season of these species lasts from March to May, which coincided with California's statewide Stay-At-Home Order (March 19 to May 4, 2020) and made them useful bio-monitors of fossil fuel emission-reductions during the period of strictest COVID-19 measures in this area.

Plant samples were collected by community scientists. These volunteers mailed the plants in paper envelopes along with the species, latitude, longitude, and date of collection. Collection dates for the samples ranged from late spring through the summer. Most plants were *Bromus tectorum* L. (cheatgrass), *Bromus diandrus* ROTH. (ripgut brome), *Avena fatua* L. (wild oat), or *Avena barbata* POTT EX LINK (slender oat). We inventoried all samples and information, confirmed their species (if identifiable), and recorded whether they were green or senesced. We also photographed all samples, focusing on their identifying features. These species represent a lower limit on annual $ffCO_2$ values since their growth period follows winter rain and wind events that cleanse pollution from the atmosphere.

We analyzed the ^{14}C content of 188 samples from the 2020 growing season and 82 samples from the 2021 growing season. For a direct comparison between the two years, we only analyzed 2021 samples that were collected within 500 m of a 2020 sample. To prepare the samples for ^{14}C analysis, we weighed out approximately 4 mg of plant tissue, focusing on flowers to target carbon fixed from the atmosphere during March to May. Samples were then sealed into pre-combusted quartz tubes with cuprous oxide, evacuated and combusted at 900°C for 3 h. The resulting CO_2 was purified cryogenically on a vacuum line, quantified manometrically, and converted to graphite using a sealed-tube zinc reduction method (Xu et al., 2007). The graphite was analyzed for ^{14}C at the W. M. Keck Carbon Cycle Accelerator Mass Spectrometer facility (NEC 0.5MV 1.5SDH-2 AMS) at the University of California, Irvine alongside processing standards and blanks. The measurement uncertainty ranged from 1.4 to 2.1‰. We use the $\Delta^{14}C$ notation (‰) for presentation of results [Eq. 1],

$$^{14}C = 1000 \quad (FM \quad \exp\left(\frac{1950 - y}{8267}\right) - 1) \quad Eq.\ 1$$

where y is the year of sampling, FM is the fraction modern calculated as the $^{14}C/^{12}C$ ratio of the sample divided by 95% of the $^{14}C/^{12}C$ ratio of the oxalic

acid (OX) I standard measured in 1950, 8267 years is the mean lifetime of ^{14}C, and 1950 is the reference year for "modern". Mass-dependent isotopic fractionation of the sample is accounted for in the fraction modern term (Trumbore et al., 2016). This ^{14}C notation includes a correction for the decay of the OX I standard since 1950, giving the absolute ^{14}C content of our samples during the year they were collected.

We used a mass balance approach (Santos et al., 2019; Turnbull et al., 2011) to quantify the fossil fuel contribution to the local CO_2 signal (C_{ff}) at each sample location. In the following equations, C_i terms denote CO_2 mixing ratios (units of ppm) from each contributing source and Δ_i terms denote the corresponding ^{14}C signature for each source in units of per mil (‰).

$$C_{obs} = C_{bg} + C_{ff} \qquad \textit{Eq. 2}$$

$$C_{obs}\Delta_{obs} = C_{bg}\Delta_{bg} + C_{ff}\Delta_{ff} \qquad \textit{Eq. 3}$$

$$C_{ff} = C_{bg}\frac{(\Delta_{bg} - \Delta_{obs})}{(\Delta_{obs} - \Delta_{ff})} \qquad \textit{Eq. 4}$$

Here, we assume the observed mixing ratio of CO_2 (units of parts per million) at a location is the sum of two contributions: the CO_2 background (C_{bg}) and a fossil fuel contribution (C_{ff}) [Eq. 2]. The isoproduct for each CO_2 source must also be conserved [Eq. 3]. Combining Equations 2 and 3, we can calculate C_{ff} for each sample [Eq. 4]. All other values are known: Δ_{obs} is the measured ^{14}C content of the plant sample. For C_{bg} we use the average CO_2 mixing ratio measured at Cape Kumukahi (Dlugokencky et al., 2021) between March and May. C_{bg} was 416.7 $\pm$ 1.1 ppm for the 2020 and 419.4 $\pm$ 0.8 ppm for the 2021 growing season, respectively. Δ_{bg} is characterized by monthly-integrated air samples collected in a remote location Pt. Barrow, Alaska (X. Xu, Pers. Comm., 2021) and was -2.8 $\pm$ 1.3‰ for the 2020 and -6.2 $\pm$ 1.7‰ for the 2021 growing season, respectively. Δ_{ff} is -1000‰, the known fossil fuel ^{14}C signature. Based on the average standard deviation of replicate plant samples and error propagation, the uncertainty in a C_{ff} estimate is 1 ppm. Our equations assume biogenic ^{14}C inputs (such as from fires or heterotrophic respiration) are small enough to be neglected in the mass balance budget. Previous work has shown that this effect is constant and relatively small (Newman et al., 2016).

3 Results and Discussion

3.1 Reduced CO_2 enhancements on Los Angeles freeways

We observed substantial reductions in on-road CO_2 enhancements (CO_{2xs}) in the LA metropolitan area during the pandemic (Fig. 1). The mean CO_{2xs} value ($\pm$ SD) on LA freeways decreased from 199 $\pm$ 42 ppm in July 2019 to 80 $\pm$ 27 ppm in July 2020, an average reduction of 60 $\pm$ 16%. CO_{2xs} reductions were universally observed across all sampled freeways. By July 2021, COVID-related restrictions were relaxed and CO_{2xs} rebounded to 233 $\pm$ 29 ppm, an average 17 $\pm$ 29% increase from 2019. The 2021 CO_{2xs} increases were not uniformly

distributed. Many freeways still had CO_{2xs} values that were lower relative to 2019, although not nearly as low as in 2020. Heavily trafficked areas had CO_{2xs} levels as much as 40% higher than 2019 (Fig S1). Furthermore, CO_{2xs} values were less variable in 2020 (interquartile range of 33 ppm) and 2021 (interquartile range of 43 ppm) compared to 2019 (58 ppm), indicating more homogeneous CO_{2xs} on roadways during the pandemic (Fig S2).
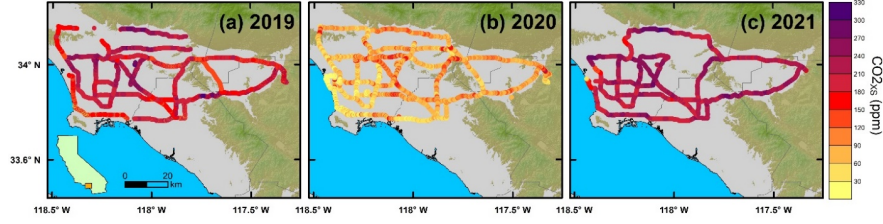

Figure 1. On-road CO_{2xs} observed near midday on Los Angeles freeways before (2019) and during the COVID-19 pandemic (2020 and 2021). Choropleth maps show CO_{2xs} observations in (a) July 2019, (b) July 2020, and (c) July 2021. Basemap shows topography for elevations >300 m as hillside shading based on a Digital Elevation Model from USGS.

Changes in traffic patterns during the pandemic are likely the main cause of the changes in on-road CO_{2xs} values we observed. Previous work has shown that on-road CO_2 mixing ratios are sensitive to traffic conditions such as speed, distance between cars and road grade (Maness et al., 2015). In July 2020, schools and businesses were operating in a remote or hybrid work model and many commercial facilities were closed, leading to substantial traffic reductions. Data from the California Department of Transportation's Performance Measurement System (PeMS) indicates that the vehicle miles traveled (VMT) on Southern California freeways was on average 12% lower in July 2020 compared to July 2019 (Caltrans, 2021). With fewer vehicles on the road in July 2020, there were wider distances between cars, fewer traffic jams, and fewer CO_2 emissions.

Nationwide studies conducted during the same period deduced that ffCO_2 emissions started recovering after reaching maximum declines in March or April of 2020, and that by July of 2020 (our study period), the reductions had largely diminished (Harkins et al., 2021; Le Quéré et al., 2020; Liu et al., 2020). Daily ground transportation emissions in the U.S. were estimated to only be reduced by 7-8% in July 2020 compared to 2019 (Harkins et al., 2021; Liu et al., 2020). Interestingly, our LA observations indicate much larger reductions to on-road CO_2 emissions during that period (~60%). This is likely because our measurements were collected in an area where emissions are dominated by passenger vehicles. In California and in LA, the transportation sector is the largest source of ffCO_2 emissions (45% of total), so changes in traffic patterns during the

pandemic were more likely to have a discernable impact on this region's ffCO$_2$ budget compared to the U.S. as a whole. A 60% decrease in on-road emissions is mathematically consistent with a previous estimate that the LA area's total emissions were reduced by 30% in the spring of 2020 relative to 2018-2019 (Yadav et al., 2021). A budget balance calculation with a 30% reduction in total LA emissions in 2020 equates to a 67% reduction in on-road emissions if we assume non-vehicle ffCO$_2$ sources were held constant and the on-road sector accounted for 45% of LA's ffCO$_2$ emissions before the pandemic. However, previous studies have shown that the pandemic-related emission reductions are not completely attributable to changes in traffic (Liu et al., 2020; Yadav et al., 2021), so our ~60% reduction result is still higher than what other studies estimated. On-road CO$_2$ measurements are likely to detect the transportation-sector emission changes with higher sensitivity than tower- and space-based observations since signal detection is not as dependent on atmospheric transport. Another study deployed a similar mobile measurement approach in Beijing, China, and observed mean CO$_{2xs}$ reductions of 41 ppm (-63% change) relative to a period before COVID-19 restrictions (Liu et al., 2021).

While our data revealed striking reductions in CO$_2$ mixing ratios, it is not trivial to translate changes in on-road CO$_2$ *mixing ratios* into reductions in CO$_2$ *emissions*. One reason for this is because of confounding effects of changes in vehicle speeds on CO$_2$ emissions. There is a nonlinear relationship between vehicle speeds and emission rates, such that vehicles emit more CO$_2$ at very low and very high speeds (Fitzmaurice et al., 2022). In 2020, our average speed was 9 km h^{-1} faster than 2019 and 12 km h^{-1} faster than 2021, which suggests a decrease in congestion in 2020. Within the range of our average speeds (64 to 76 km/hr), there is not expected to be a substantial change in CO$_2$ emission rates (Fitzmaurice et al., 2022). However, these averages do not capture the non-constant speeds during periods of congestion that make vehicles less efficient and increase both CO$_2$ emissions and mixing ratios. On the other hand, faster speeds produce more CO$_2$ emissions because vehicle engines are doing more work and using more fuel. But they also create more turbulence near the road that effectively mixes CO$_2$, thereby reducing on-road CO$_2$ mixing ratios. Nonetheless, we did not find a significant relationship between our measurements of CO$_{2xs}$ and vehicle speed (Fig S3). We estimated how much vehicle speed would affect our measurements using a model where on-road CO$_{2xs}$ levels scale with vehicle speed to a power of - (Baker, 1996; Maness et al., 2015). Assuming that total highway emissions (Q) are related to CO$_{2xs}$ and vehicle speed (v) by Equation 5 where is a constant of proportionality based on theoretical atmosphere and traffic conditions, a 9 km/hr increase in speed like we saw in 2020 only causes total emissions to increase by less than 5%. Thus, we conclude that the CO$_{2xs}$ reductions we measured are more likely a result of decreased emissions from the reduced number of cars on the road, not changes in speed.

$$\overline{\overline{CO_{2xs} =\ Q\ v^{-1/3}\quad \textit{Eq. 5}}}$$

Interestingly, our on-road observations did not scale proportionally with vehicle miles traveled (VMT), a commonly used metric for inferring $ffCO_2$ emissions. While we observed a $60 \pm 16\%$ reduction in CO_{2xs} in July 2020 relative to July 2019, VMT in the LA area was only reduced by 12% during the same time periods (CalTrans, 2021). Thus, VMT does not adequately capture the strong signal we observed. Recent studies have reported severe discrepancies between $ffCO_2$ emission estimates based on governmental traffic data, fuel-based models, and novel cell phone-based mobility datasets (Gensheimer et al., 2021; Harkins et al., 2021; Oda et al., 2021). Future work is needed to consolidate these different metrics for estimating transportation $ffCO_2$ emissions and to better understand what information each of these datasets represent.

Assuming the measured 60% reduction in on-road CO_{2xs} translates into a 60% reduction in annual interstate $ffCO_2$ emissions (7.6 Mt C yr^{-1} in 2012; Rao et al., 2017), this equates to an avoided 4.6 Mt C. The estimated total emissions for the LA area were 48.06 ± 5.3 Mt C yr^{-1} in 2011 (Gurney et al., 2019). This would imply that LA's total $ffCO_2$ emissions were reduced by 10% if all of the pandemic-induced reductions in 2020 were solely due to changes to on-road interstate emissions. Interstate emissions constitute only 40% of LA's on-road emissions (Rao et al., 2017). If we instead assume the COVID-induced traffic reductions resulted in a 60% reduction in $ffCO_2$ for the entire on-road sector (including all road types), then $ffCO_2$ emissions were reduced by 11.4 Mt C, or 24% of LA's total $ffCO_2$ emissions.

These large CO_{2xs} reductions indicate that reforming California's mobility patterns is a crucial pathway toward mitigating CO_2 emissions. Electrification of California's vehicle fleet is underway, with recent state policies demanding the phase out of gas-powered vehicles within the next few decades (e.g., SB 500, Executive Order N-79-20). Increasing flexibility in remote work could be an impactful mitigation strategy by ultimately reducing the number of vehicle miles traveled. This would require a significant investment in internet and power accessibility.

3.2 Reduced statewide $ffCO_2$ emissions during COVID-19

[14]C analyses of plant species were used to map $ffCO_2$ patterns during the pandemic, where lower ^{14}C values indicate higher $ffCO_2$ inputs (Fig. 2). In 2020, the average [14]C ($\pm$ SD) was -11.3 $\pm$ 8.6‰ (n=188) statewide, and -15.9 $\pm$ 12.5‰ (n=53) in the LA area, -10.2 $\pm$ 5.5‰ (n=91) in the San Francisco Bay Area (SFBA), and -10.3 $\pm$ 5.6‰ (n=12) in the San Joaquin Valley. This equates to average fossil fuel contributions of 3.6 $\pm$ 3.8 ppm statewide, and 5.6 $\pm$ 5.5 ppm in the LA area, 3.1 $\pm$ 2.3 ppm in the SFBA, and 3.2 $\pm$ 2.3 ppm in the San Joaquin Valley. The cleanest samples (most enriched in ^{14}C) were found in California's northern coast (^{14}C of -5.3 $\pm$ 3.7‰, n = 5). Generally, ^{14}C of plants collected in urban areas were more depleted and more variable, indicating higher and locally variable emissions of $ffCO_2$.
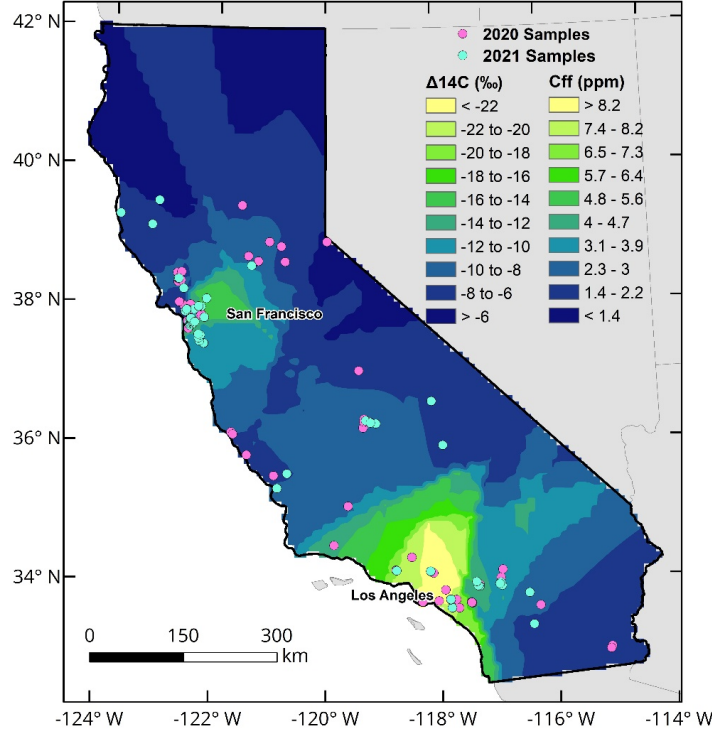
Figure 2. The ^{14}C (‰) of annual grass samples collected in California, USA and the corresponding C$_{ff}$ values in 2020. Blue points indicate locations where plants were collected in both 2020 and 2021, while pink points indicate 2020-only locations. Background colors were mapped using an ordinary kriging interpolation of 2020 plant ^{14}C values using the Spatial Analyst toolbox in ESRI's ArcMap software.

Although the pandemic continued into the 2021 growing season, virus-restricting mandates were relaxed and California's vehicle miles traveled were 30% higher than the same period in 2020 (Caltrans, 2021). We observed large spatial variations and heterogeneity in ^{14}C during the second spring and summer of the pandemic. ^{14}C was on average 4.8 ± 7.8‰ more depleted in 2021 than in 2020, based on a subset of samples collected near the same locations in both years (< 500 m away). However, this ^{14}C decline cannot be attributed to changes in human behavior during COVID-19 because global atmospheric ^{14}C has been linearly declining at an approximate rate of -5‰ y^{-1} since the 1990's (Graven

11

et al., 2020). In terms of C_{ff}, the statewide mean difference between the two years was only 0.7 ppm, which is below our estimated uncertainty of 1 ppm C_{ff}. Regionally, there was a mean difference between 2021 and 2020 of 2.7 $\pm$ 4.0 ppm for the LA sample pairs (n = 18), -0.1 $\pm$ 3.0 ppm for the SFBA (n = 32), and -1.4 $\pm$ 1 ppm for the San Joaquin Valley (n=4).

Despite the seemingly small change at the state and regional scale, there was substantial *local* variability in the changes in ^{14}C between 2020 and 2021 (Fig. S4). For the growing season which our samples represent, the background ^{14}C decreased by 3.5 ‰ from 2020 to 2021. 49% of the re-samples (n=29) were depleted by more than 3.5‰, indicating increased ffCO$_2$ emissions at these locations in 2021. 24% samples (n=14) were depleted by less than 3.5‰, suggesting a negligible local difference in ffCO$_2$ between 2020 and 2021. 27% of samples (n=16) were enriched in ^{14}C relative to 2020, which implies that ffCO$_2$ emission reductions persisted into 2021 in these locations and local air was cleaner than in 2020. Another factor for cases where the 2020 sample was more polluted than 2021 is that a portion of the carbon in the 2020 plant samples could have been fixed from the atmosphere prior to the imposition of the Stay-At-Home order on March 19, 2020. Solar induced fluorescence (SIF) measurements indicate the photosynthetic uptake period of annual grasses ranges from January to June, but peaks between March and May for regions of the state where samples were taken (Fig. S6). Ultimately however, we assume that differences in ^{14}C values are mainly driven by changes in fossil fuel consumption after the start of the Stay-At-Home order since we sampled the most recently grown plant tissue (flowers).

This disparity in ffCO$_2$ emission rebounds in 2021 could be related to regional variation in pandemic responses. We observed larger emission rebounds in LA than SFBA (Fig. 3). SFBA had more instances of ^{14}C values that either increased or only decreased as much as the long-term global ^{14}C trend between 2020 and 2021. The SFBA had a slower relaxation of COVID-19 prevention measures than other regions of California. For instance, the Great Highway, a major north-south thoroughfare on San Francisco's western edge, was closed to vehicles from April 2020 to August 2021. The road was converted into a car-free active transportation route, with access permitted only to pedestrians and bicyclists. Vehicle traffic was rerouted to 19th Avenue, a portion of CA State Route 1 less than 3 km east of the Great Highway. In 2020, plants collected along these two roads had very similar ^{14}C values (0.8‰ difference, which is within the measurement uncertainty). In 2021, a plant collected in the Great Highway was still statistically indistinguishable from the 2020 samples (0.7‰ difference), while a plant sample collected on 19th Avenue was significantly more depleted relative to the 2020 sample (-24.8‰ difference, equivalent to an increase of 10 ppm C_{ff}). This indicates higher ffCO$_2$ emissions on 19th Avenue where traffic increased in 2021, while ffCO$_2$ emission reductions near the Great Highway persisted while the roadway remained closed to vehicles.
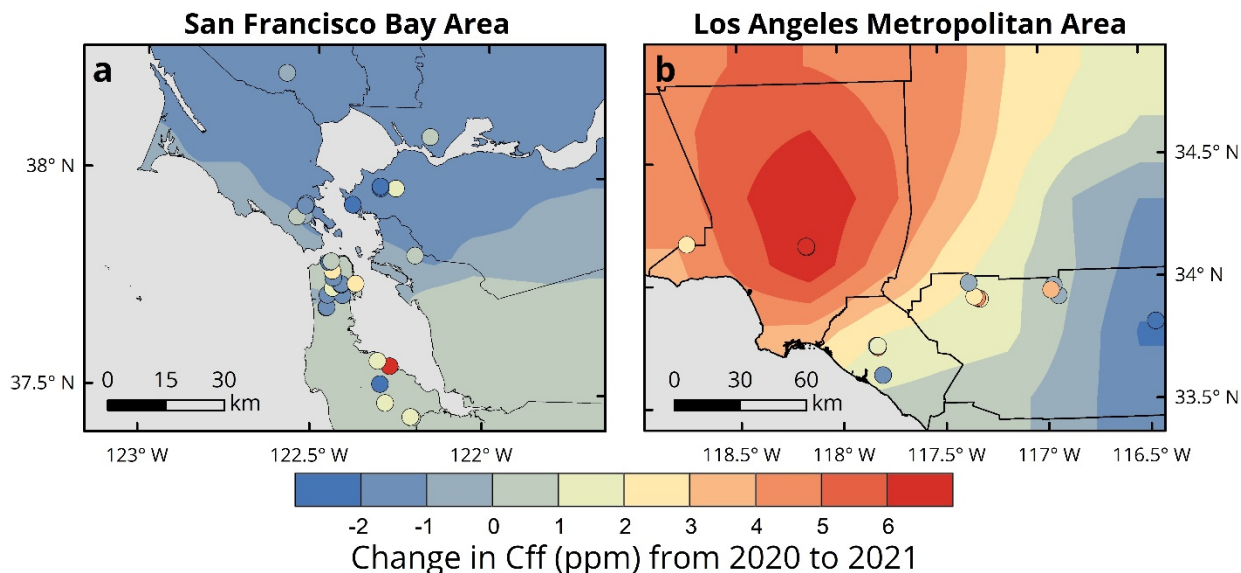
San Francisco Bay Area

Los Angeles Metropolitan Area

Change in Cff (ppm) from 2020 to 2021

Figure 3. The difference in C_{ff} values from 2020 to 2021 between plant samples repeatedly collected in California's urban areas: (a) the San Francisco Bay Area and (b) the Los Angeles metropolitan area. Redder colors indicate ffCO$_2$ emission increases in 2021 compared to 2020. Background colors were calculated using an Ordinary Kriging interpolation of C_{ff} in ESRI's ArcMap software. Points show sample locations colored by their change in Cff.

We estimated ffCO$_2$ emission reductions in Pasadena (a city in the northeast LA basin) by comparing the ^{14}C of a 2020 plant sample to extrapolated measurements of ambient ^{14}CO$_2$ collected at the California Institute of Technology between 2006 to 2013 (Newman et al., 2016) (Fig. 4). Pasadena tends to have enhanced CO$_2$ levels since prevailing winds bring in polluted air from LA that gets trapped by the San Gabriel Mountains. Based on a linear extrapolation of the Pasadena air record, the mean ^{14}C during the 2020 growing season would have been -55.5 $\pm$ 8.8‰ had there been no pandemic, translating to a local enhancement of 23 ppm CO$_2$ above background [Eq. 4]. Since plants integrate carbon into their tissue over the entire growing season, plant ^{14}C should be representative of ambient ^{14}CO$_2$ averaged over the growing season (March to May). A plant sample collected approximately 4 km away had an enhancement of only 3 ppm CO$_2$ above background. Thus, this 45‰ discrepancy in ^{14}C equates to a reduction of 19 $\pm$ 12 ppm ffCO$_2$ based on the sensitivity of ^{14}C to fossil fuel inputs of -2.4‰ per ppm ffCO$_2$ in the year 2020. In 2021, plants were sampled in this location again and had an average ^{14}C of -35.7 $\pm$ 4.5 ‰ (n=6), an enhancement of 13 ppm CO$_2$. This value is closer to, but still significantly different from, the predicted 2021 mean value (-60 $\pm$ 9.4‰ or 22 ppm CO$_2$ enhancement), indicating a partial but not complete rebound to the pre-pandemic

13

emissions trend. In summary, we found that plant ^{14}C data was able to capture interannual changes in ffCO$_2$ at the neighborhood scale in response to changes in traffic patterns.
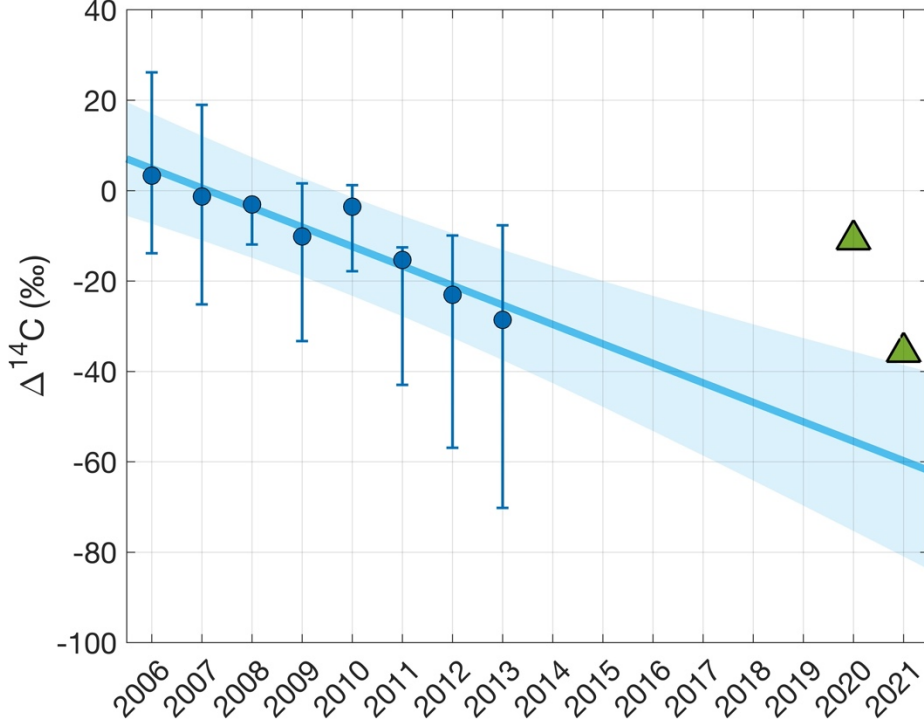

Figure 4. Δ^{14}C of ambient CO$_2$ in Pasadena, CA, a city within the northeast Los Angeles basin. The blue circles show the average growing season Δ^{14}C of ambient CO$_2$ at Caltech [*Newman et al., 2016*], with error bars showing the minimum and maximum Δ^{14}C measurements. The line is a linear regression of these data with shading indicating the 95% confidence intervals. The green triangles show the measured Δ^{14}C of plant samples collected approximately 4 km away from the Caltech site in 2020 and 2021.

3.3 Long-term changes in California's ffCO$_2$ emissions

To assess our plant ^{14}C observations in the context of long-term trends in the region, we compared our dataset to existing records of plant and air ^{14}CO$_2$ analyses (Fig. 5). The global decline in ambient ^{14}CO$_2$ is evident in ^{14}CO$_2$ samples from both Irvine, CA (a coastal city south of LA) and Pt. Barrow, AK (a remote location far from ffCO$_2$ sources). The slope of a linear fit of the Pt. Barrow annual averages indicates that the background atmospheric ^{14}C content is declining by 4.2‰ yr^{-1}. In more recent years (post-2018), this trend has slowed down to 2.5‰ yr^{-1}. For growing season observations only, the background ^{14}C decreased by 3.5 ‰ from 2020 to 2021 while the statewide means of our ^{14}C samples decreased by 5.3 ± 15‰.
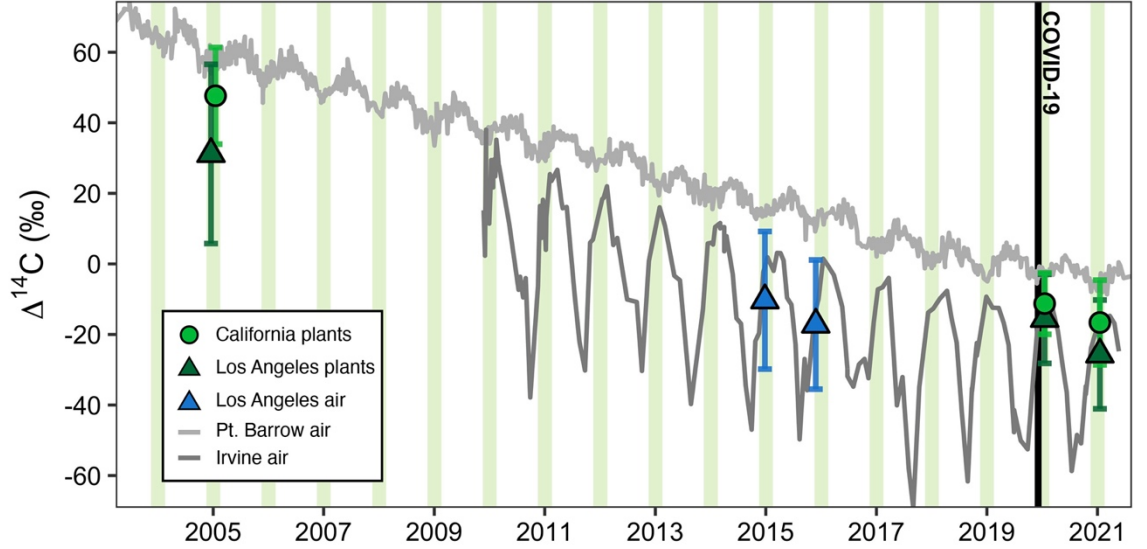
14

Figure 5. A record of ^{14}C measurements from 2003-2021. Average plant ^{14}C from various studies are shown as green points with error bars showing the standard deviation. Green circles represent statewide data (this study and Riley et al. 2008) while triangles represent only the Los Angeles metropolitan area (this study and Wang & Pataki, 2010). Air-based ^{14}C observations are shown as gray lines (X. Xu, Pers. Comm., 2021) and blue triangles (Miller et al., 2020). Shaded green bars represent the typical annual grass growing season in California (March to May).

We infer urban ffCO$_2$ emission reductions relative to the ^{14}C records shown in Fig. 5 based on two metrics: variability in [14]C (standard deviation of sample mean) and the difference in ^{14}C from background (Pt. Barrow, Alaska). Reduced variability in ^{14}C indicates reduced ffCO$_2$ levels since emissions lead to anomalous and spatially variable ^{14}C values. The standard deviations of plant ^{14}C samples collected in the LA metropolitan area were 25.4‰ in 2005 (n=79, Wang & Pataki, 2010), 12.5‰ in 2020 (n=53), and 15.4‰ in 2021 (n=27). Thus, plant ^{14}C was less variable in 2020 during California's Stay-At-Home order than in other years.

Furthermore, 2020 samples were the least ^{14}C-depleted from the background relative to samples from other years. In the LA metropolitan area, ^{14}C samples were depleted by 26 ± 3‰ in 2005 (Wang & Pataki, 2010), 25 ± 2‰ in 2015, 30 ± 4‰ in 2016 (Miller et al., 2020), 13 ± 2‰ in 2020, and 19 ± 3‰ in 2021 (average ± standard error of the mean). The mean 2020 depletion is significantly different from pre-pandemic years to a 95% confidence interval, indicating that 2020 was an exceptionally clean year.

Translating the ^{14}C depletion from background into fossil fuel-sourced CO$_2$ en-

hancements (C_{ff} in Eq. 4), the mean C_{ff} in LA was 5.6 ± 5.5 ppm in 2020. This value is 43-55% lower than the mean C_{ff} of pre-pandemic years, which ranged from 10-13 ppm. Thus, we calculate that a 10-24% reduction in LA's $ffCO_2$ emissions during the COVID-19 pandemic (based on on-road emission reductions calculated in Section 3.1), resulted in a 43-55% plant ^{14}C signal relative to pre-pandemic observations.

Plant ^{14}C analysis captured trends in ambient $^{14}CO_2$, with plant values having reasonable correspondence with air records from Irvine, CA and Pt. Barrow, AK (Fig. 5), demonstrating the potential of plants to serve as time-integrated ^{14}C monitors for global cities. The ^{14}C content of managed turfgrass also coincided with the ^{14}C measured by a rooftop air monitoring site less than 1 km away (Fig. S5), supporting the idea that intermittent sampling of plants could potentially be used to track temporal trends in atmospheric ^{14}C at sub-annual scales. Preparation for ^{14}C analysis is significantly faster for plant samples and can be done with just 4 mg of plant tissue since plants are approximately 40% C, while air samples ($< 0.0415\%$ C) require expensive canisters and larger volume samples (~6 L) and longer processing times to get a large enough ^{14}C sample for AMS analysis. This means that more ^{14}C samples can be analyzed leading to higher resolution and easier-to-interpret urban $ffCO_2$ datasets than with air samples.

Atmospheric $^{14}CO_2$ undergoes large temporal oscillations (Fig. 5) with the amplitude and seasonality driven by the timing of ^{14}C production and descendance into the troposphere, natural and anthropogenic CO_2 fluxes, and seasonal meteorology (wind and air mixing conditions). Thus, it is important to constrain the timing of carbon uptake as much as possible to distinguish spatially driven changes from temporal changes. While the timing of flask sample collection is well-known, the timing of CO_2 uptake by plants is more uncertain. However, plant samples compensate for that by integrating over daytime hours of their photosynthetic period, hence, reducing significant short-term variability observed in flask samples (e.g., Miller et al., 2020) to yield a seasonal average $ffCO_2$.

By sampling annual grasses, we have assumed that our ^{14}C analysis represents the growing season of these species in the region. We verified this assumption using downscaled remotely sensed observations of solar induced fluorescence (SIF) (Turner et al., 2020b) from the TROPOMI instrument onboard the Sentinel-5 Precursor satellite. We used the date of maximum SIF to represent the timing of peak growth for senesced plant samples. In accordance with our assumption, we found that all senesced plants had peak growth dates from March to May. Using the date of maximum SIF observance to represent the timing of peak growth, we found some temporal agreement between plant ^{14}C and ambient $^{14}CO_2$ measured in Irvine, CA (Fig. S6), suggesting potential applications of plant ^{14}C at the sub-seasonal scale. However, many ^{14}C values did not coincide with the Irvine trend and were more strongly driven by their distance to major roads (Fig. S6c), showing that the main driver of the samples' ^{14}C content is

proximity to ffCO$_2$ emissions, on top of seasonality. Weather patterns such as wind speed, wind direction and storms affect how CO$_2$ spreads or accumulates from emission sources, and thus impact local ffCO$_2$ levels. In the springtime, winds in the LA area are mainly expected to originate offshore (westerly flow), with occasional reversal ("Santa Ana" conditions) (Verhulst et al., 2017). Here, we expect that the plant samples experienced similar meteorological conditions across both study years. SIF observations can help constrain the timing of plant growth for future studies to disentangle the spatial and temporal drivers of plant ^{14}C. Future studies could potentially use purposely grown plants to monitor ffCO$_2$, and actively manage the growing period to the timing of interest, which would allow similar analyses at smaller time scales and for other times of the year besides the annual grass growing season.

5 Conclusions

We assessed changes in fossil fuel consumption during the first two years of the COVID-19 pandemic (2020 to 2021) using on-road CO$_2$ observations on freeways and ^{14}C analysis of annual plants collected by community scientists. Both measurements detected large reductions in fossil CO$_2$ emissions in 2020 and varying degrees of emission recovery by 2021. The strengths of these approaches for future ffCO$_2$ monitoring applications were evident. Unlike tower-top measurements of CO$_2$ mole fractions, our datasets can be unambiguously linked to emission sources (on-road sector and fossil fuels), are time-integrated, and have a higher spatial resolution than tower networks, which require expensive and accessible infrastructure, and complex atmospheric transport modeling to partition sources and map spatial patterns. The sensitivity of plant ^{14}C to changes in fossil fuel consumption during the pandemic imply that plants may serve as cost-effective monitors of ffCO$_2$ emission patterns in places without established monitoring infrastructure, such as growing cities in the Global South.

Despite the drastic changes in ffCO$_2$ emissions we observed in California, these reductions did not slow the global atmospheric growth rate of CO$_2$ (Laughner et al., 2021). While there were large reductions, the emissions rebounded relatively quickly to pre-pandemic levels. Larger-scale and persistent change is needed to make lasting reductions to global ffCO$_2$ emissions and mitigate climate change.

Conflict of Interest Statement

The authors declare no conflicts of interest.

Open Research

The datasets of on-road CO_2 and plant radiocarbon are available in the Dryad public data repository and can be accessed via https://doi.org/10.7280/D1F98G (Yañez et al., 2022).

References

Baker, C. J. (1996). Outline of a novel method for the prediction of atmospheric pollution dispersal from road vehicles. *Journal of Wind Engineering and Industrial Aerodynamics*, *65*, 395–404.

Buchwitz, M., Reuter, M., Noël, S., Bramstedt, K., Schneising, O., Hilker, M., Fuentes Andrade, B., Bovensmann, H., Burrows, J. P., di Noia, A., Boesch, H., Wu, L., Landgraf, J., Aben, I., Retscher, C., O'Dell, C. W., & Crisp, D. (2021). Can a regional-scale reduction of atmospheric CO2during the COVID-19 pandemic be detected from space? A case study for East China using satellite XCO2 retrievals. *Atmospheric Measurement Techniques*, *14*(3), 2141–2166. https://doi.org/10.5194/amt-14-2141-2021

Bush, S. E., Hopkins, F. M., Randerson, J. T., Lai, C. T., & Ehleringer, J. R. (2015). Design and application of a mobile ground-based observatory for continuous measurements of atmospheric trace gas and criteria pollutant species. *Atmospheric Measurement Techniques*, *8*(8), 3481–3492. https://doi.org/10.5194/amt-8-3481-2015

Caltrans, California Department of Transportation. (2021). Caltrans, California Department of transportation. Performance Measurement System Data Source. Retrieved from http://pems.dot.ca.gov/

Carranza, V., Biggs, B., Meyer, D., Townsend-Small, A., Thiruvenkatachari, R. R., Venkatram, A., Fischer, M. L., & Hopkins, F. M. (2022). Isotopic Signatures of Methane Emissions From Dairy Farms in California's San Joaquin Valley. *Journal of Geophysical Research: Biogeosciences*, *127*(1), 1–15. https://doi.org/10.1029/2021JG006675

Chevallier, F., Zheng, B., Broquet, G., Ciais, P., Liu, Z., Davis, S. J., Deng, Z., Wang, Y., Bréon, F. M., & O'Dell, C. W. (2020). Local Anomalies in the Column-Averaged Dry Air Mole Fractions of Carbon Dioxide Across the Globe During the First Months of the Coronavirus Recession. *Geophysical Research Letters*, *47*(22). https://doi.org/10.1029/2020GL090244

Dlugokencky, E.J., J.W. Mund, A.M. Crotwell, M.J. Crotwell, and K.W. Thoning (2021), Atmospheric Carbon Dioxide Dry Air Mole Fractions from the NOAA GML Carbon Cycle Cooperative Global Air Sampling Network, 1968-2020, Version: 2021-07-30, https://doi.org/10.15138/wkgj-f215

Duren, R. M., & Miller, C. E. (2012). Measuring the carbon emissions of megacities. In *Nature Climate Change* (Vol. 2, Issue 8, pp. 560–562). Nature Pub-

lishing Group. https://doi.org/10.1038/nclimate1629

Eldering, A., Taylor, T. E., O'Dell, C. W., & Pavlick, R. (2019). The OCO-3 mission: Measurement objectives and expected performance based on 1 year of simulated data. *Atmospheric Measurement Techniques*, *12*(4), 2341–2370. https://doi.org/10.5194/amt-12-2341-2019

Fitzmaurice, H. L., Turner, A. J., Kim, J., Chan, K., Delaria, E. R., Newman, C., Wooldridge, P., & Cohen, R. C. (2022). Assessing vehicle fuel efficiency using a dense network of CO2 observations. *Atmospheric Chemistry and Physics*, *22*(6), 3891–3900. https://doi.org/10.5194/acp-22-3891-2022

Gensheimer, J., Turner, A. J., Shekhar, A., Wenzel, A., Keutsch, F. N., & Chen, J. (2021). What Are the Different Measures of Mobility Telling Us About Surface Transportation CO2 Emissions During the COVID-19 Pandemic? *Journal of Geophysical Research: Atmospheres*, *126*(11), 1–11. https://doi.org/10.1029/2021JD034664

Graven, H., Keeling, R. F., & Rogelj, J. (2020). Changes to Carbon Isotopes in Atmospheric CO2 Over the Industrial Era and Into the Future. *Global Biogeochemical Cycles*, *34*(11), 1–21. https://doi.org/10.1029/2019GB006170

Gurney, K. R., Patarasuk, R., Liang, J., Song, Y., O'Keeffe, D., Rao, P., Whetstone, J. R., Duren, R. M., Eldering, A., & Miller, C. (2019). The Hestia Fossil Fuel CO2 Emissions Data Product for the Los Angeles Megacity (Hestia-LA). *Earth System Science Data Discussions*, 1–38. https://doi.org/10.5194/essd-2018-162

Harkins, C., McDonald, B. C., Henze, D. K., & Wiedinmyer, C. (2021). A fuel-based method for updating mobile source emissions during the COVID-19 pandemic. *Environmental Research Letters*, *16*(6). https://doi.org/10.1088/1748-9326/ac0660

Hopkins, F. M., Kort, E. A., Bush, S. E., Ehleringer, J. R., Lai, C.-T., Blake, D. R., & Randerson, J. T. (2016). Spatial patterns and source attribution of urban methane in the Los Angeles basin. *Journal of Geophysical Research: Atmospheres*, *121*(5), 2490–2507. https://doi.org/10.1002/2015JD024429.Received

Hsueh, D. Y., Krakauer, N. Y., Randerson, J. T., Xu, X., Trumbore, S. E., & Southon, J. R. (2007). Regional patterns of radiocarbon and fossil fuel-derived CO2 in surface air across North America. *Geophysical Research Letters*, *34*(2), L02816.

Kiel, M., Eldering, A., Roten, D. D., Lin, J. C., Feng, S., Lei, R., Lauvaux, T., Oda, T., Roehl, C. M., Blavier, J. F., & Iraci, L. T. (2021). Urban-focused satellite CO2 observations from the Orbiting Carbon Observatory-3: A first look at the Los Angeles megacity. *Remote Sensing of Environment*, *258*(January). https://doi.org/10.1016/j.rse.2021.112314

Laughner, J. L., Neu, J. L., Schimel, D., Wennberg, P. O., Barsanti, K., Bowman, K. W., Chatterjee, A., Croes, B. E., Fitzmaurice, H. L., Henze, D. K.,

Kim, J., Kort, E. A., Liu, Z., Miyazaki, K., Turner, A. J., Anenberg, S., Avise, J., Cao, H., Crisp, D., … Zeng, Z. (2021). Societal shifts due to COVID-19 reveal large-scale complexities and feedbacks between atmospheric chemistry and climate change. *Proceedings of the National Academy of Sciences*, *118*(46). https://doi.org/10.1073/pnas.2109481118/-/DCSupplemental.Published

Le Quéré, C., Jackson, R. B., Jones, M. W., Smith, A. J. P., Abernethy, S., Andrew, R. M., De-Gol, A. J., Willis, D. R., Shan, Y., Canadell, J. G., Friedlingstein, P., Creutzig, F., & Peters, G. P. (2020). Temporary reduction in daily global CO2 emissions during the COVID-19 forced confinement. *Nature Climate Change*, 1–7. https://doi.org/10.1038/s41558-020-0797-x

Le Quéré, C., Peters, G. P., Friedlingstein, P., Andrew, R. M., Canadell, J. G., Davis, S. J., Jackson, R. B., & Jones, M. W. (2021). Fossil CO2 emissions in the post-COVID-19 era. *Nature Climate Change*, *11*(3), 197–199. https://doi.org/10.1038/s41558-021-01001-0

Liu, D., Sun, W., Zeng, N., Han, P., Yao, B., Liu, Z., Wang, P., Zheng, K., Mei, H., & Cai, Q. (2021). Observed decreases in on-road CO2 concentrations in Beijing during COVID-19 restrictions. *Atmospheric Chemistry and Physics*, *21*(6), 4599–4614. https://doi.org/10.5194/acp-21-4599-2021

Liu, Z., Ciais, P., Deng, Z., Lei, R., Davis, S. J., Feng, S., Zheng, B., Cui, D., Dou, X., Zhu, B., Guo, R., Ke, P., Sun, T., Lu, C., He, P., Wang, Y., Yue, X., Wang, Y., Lei, Y., … Schellnhuber, H. J. (2020). Near-real-time monitoring of global CO2 emissions reveals the effects of the COVID-19 pandemic. *Nature Communications*, *11*(1), 1–12. https://doi.org/10.1038/s41467-020-18922-7

Maness, H. L., Thurlow, M. E., McDonald, B. C., & Harley, R. A. (2015). Estimates of CO2 traffic emissions frommobile concentration measurements. *Journal of Geophysical Research*, *120*(5), 2087–2102. https://doi.org/10.1002/2014JD022876

Miller, J. B., Lehman, S. J., Verhulst, K. R., Miller, C. E., Duren, R. M., Yadav, V., Newman, S., & Sloop, C. D. (2020). Large and seasonally varying biospheric CO2 fluxes in the Los Angeles megacity revealed by atmospheric radiocarbon. *Proceedings of the National Academy of Sciences of the United States of America*, *117*(43), 26681–26687. https://doi.org/10.1073/pnas.2005253117

Newman, S., Xu, X., Gurney, K. R., Hsu, Y. K., Li, K. F., Jiang, X., Keeling, R. F., Feng, S., O'Keefe, D., & Patarasuk, R. (2016). Toward consistency between trends in bottom-up CO2 emissions and top-down atmospheric measurements in the Los Angeles megacity. *Atmospheric Chemistry and Physics*, *16*(6), 3843–3863.

Oda, T., Haga, C., Hosomi, K., Matsui, T., & Bun, R. (2021). Errors and uncertainties associated with the use of unconventional activity data for estimating CO2 emissions: The case for traffic emissions in Japan. *Environmental Research Letters*, *16*(8). https://doi.org/10.1088/1748-9326/ac109d

Rao, P., R. Gurney, K., Patarasuk, R., Song, Y., E. Miller, C., M. Duren, R., & Eldering, A. (2017). Spatio-temporal Variations in on-road CO2 Emissions in the Los Angeles Megacity. *AIMS Geosciences*, *3*(2), 239–267. https://doi.org/10.3934/geosci.2017.2.239

Riley, W. J., Hsueh, D. Y., Randerson, J. T., Fischer, M. L., Hatch, J. G., Pataki, D. E., Wang, W., & Goulden, M. L. (2008). Where do fossil fuel carbon dioxide emissions from California go? An analysis based on radiocarbon observations and an atmospheric transport model. *Journal of Geophysical Research: Biogeosciences*, *113*(G4).

Rosenzweig, C., Solecki, W., Hammer, S. A., & Mehrotra, S. (2010). Cities lead the way in climate-change action. *Nature*, *467*(7318), 909–911. https://doi.org/10.1038/467909a

Santos, G. M., Oliveira, F. M., Park, J., Sena, A. C. T., Chiquetto, J. B., Macario, K. D., & Grainger, C. S. G. (2019). Assessment of the regional fossil fuel CO2 distribution through Δ14C patterns in ipê leaves: The case of Rio de Janeiro state, Brazil. *City and Environment Interactions*, *1*, 100001. https://doi.org/10.1016/j.cacint.2019.06.001

Schwandner, F. M., Gunson, M. R., Miller, C. E., Carn, S. A., Eldering, A., Krings, T., Verhulst, K. R., Schimel, D. S., Nguyen, H. M., Crisp, D., O'Dell, C. W., Osterman, G. B., Iraci, L. T., & Podolske, J. R. (2017). Spaceborne detection of localized carbon dioxide sources. *Science*, *358*(6360). https://doi.org/10.1126/science.aam5782

Seto, K. C., Dhakal, S., Bigio, A., Blanco, H., Delgado, G. C., De- war, D., Huang, L., Inaba, A., Kansal, A., Lwasa, S., McMahon, J., Muller, D. B., Murakami, J., Nagendra, H., & Ramaswami, A. (2014). Human Settlements, Infrastructure, and Spatial Planning. *Climate Change 2014 Mitigation of Climate Change. Contribution of Working Group III Too the Fifth Assessment Report of the Intergovernmental Panel on Climate Change*, 923–1000. https://doi.org/10.1017/cbo9781107415416.018

Thiruvenkatachari, R. R., Carranza, V., Ahangar, F., Marklein, A., Hopkins, F., & Venkatram, A. (2020). Uncertainty in using dispersion models to estimate methane emissions from manure lagoons in dairies. *Agricultural and Forest Meteorology*, *290*. https://doi.org/10.1016/j.agrformet.2020.108011

Turnbull, J. C., Karion, A., Fischer, M. L., Faloona, I., Guilderson, T., Lehman, S. J., Miller, B. R., Miller, J. B., Montzka, S., Sherwood, T., Saripalli, S., Sweeney, C., & Tans, P. P. (2011). Assessment of fossil fuel carbon dioxide and other anthropogenic trace gas emissions from airborne measurements over Sacramento, California in spring 2009. *Atmospheric Chemistry and Physics*, *11*(2), 705–721. https://doi.org/10.5194/acp-11-705-2011

Turner, A. J., Kim, J., Fitzmaurice, H., Newman, C., Worthington, K., Chan, K., Wooldridge, P. J., Köehler, P., Frankenberg, C., & Cohen, R. C. (2020). Ob-

served Impacts of COVID-19 on Urban CO2 Emissions. *Geophysical Research Letters*, *47*(22), 1–6. https://doi.org/10.1029/2020GL090037

Turner, A. J., Köhler, P., Magney, T. S., Frankenberg, C., Fung, I., & Cohen, R. C. (2020). A double peak in the seasonality of California's photosynthesis as observed from space. *Biogeosciences*, *17*(2), 405–422. https://doi.org/10.5194/bg-17-405-2020

Verhulst, K. R., Karion, A., Kim, J., Salameh, P. K., Keeling, R. F., Newman, S., Miller, J., Sloop, C., Pongetti, T., Rao, P., Wong, C., Hopkins, F. M., Yadav, V., Weiss, R. F., Duren, R. M., & Miller, C. E. (2017). Carbon dioxide and methane measurements from the Los Angeles Megacity Carbon Project – Part 1: calibration, urban enhancements, and uncertainty estimates. *Atmospheric Chemistry and Physics*, *17*(13), 8313–8341. https://doi.org/10.5194/acp-17-8313-2017

Wang, W., & Pataki, D. E. (2010). Spatial patterns of plant isotope tracers in the Los Angeles urban region. *Landscape Ecology*, *25*(1), 35–52. https://doi.org/10.1007/s10980-009-9401-5

Ware, J., Kort, E. A., DeCola, P., & Duren, R. (2016). Aerosol lidar observations of atmospheric mixing in Los Angeles: Climatology and implications for greenhouse gas observations. *Journal of Geophysical Research*, *121*(16), 9862–9878. https://doi.org/10.1002/2016JD024953

Yañez, C. C., Hopkins, F. M., Xu, X., Tavares, J. F., Welch, A. M., & Czimczik, C. I. (2022), Reductions in California's urban fossil fuel CO2 emissions during the COVID-19 pandemic [Dataset]. Dryad. https://doi.org/10.7280/D1F98G

Yadav, V., Ghosh, S., Mueller, K., Karion, A., Roest, G., Gourdji, S., Lopez-Coto, I., Gurney, K., Parazoo, N., Verhuslt, K. R., Kim, J., Prinzivalli, S., Fain, C., Nehrkorn, T., Mountain, M. E., Keeling, R. F., Weiss, R. F., Duren, R., Miller, C. E., & Whetstone, J. (2021). The Impact of COVID-19 on CO2 Emissions in the Los Angeles and Washington DC/Baltimore Metropolitan Areas. *Geophysical Research Letters*, *48*(11). https://doi.org/https://doi.org/10.1029/2021GL092744

Zheng, B., Geng, G., Ciais, P., Davis, S. J., Martin, R. v., Meng, J., Wu, N., Chevallier, F., Broquet, G., Boersma, F., van Der, R. A., Lin, J., Guan, D., Lei, Y., He, K., & Zhang, Q. (2020). Satellite-based estimates of decline and rebound in China's CO2 emissions during COVID-19 pandemic. *Science Advances*, *6*(49). https://doi.org/10.1126/sciadv.abd4998

Zhou, Y., Smith, S. J., Zhao, K., Imhoff, M., Thomson, A., Bond-Lamberty, B., Asrar, G. R., Zhang, X., He, C., & Elvidge, C. D. (2015). A global map of urban extent from nightlights. *Environmental Research Letters*, *10*(5), 2000–2010. https://doi.org/10.1088/1748-9326/10/5/054011